

# Lasing with well-defined cavity modes in dye-infiltrated silica inverse opals

Yoshiaki Nishijima, Kosei Ueno, Saulius Juodkazis, Vygantas Mizeikis, Hideki Fujiwara, Keiji Sasaki, and Hiroaki Misawa\*

Research Institute for Electronic Science (RIES), Hokkaido University, CRIS Bldg., Kita 21 Nishi 10, Kita-ku Sapporo 001-0021, Japan  
[misawa@es.hokudai.ac.jp](mailto:misawa@es.hokudai.ac.jp)

**Abstract:** Lasing in dye solution-embedded inverse silica opal structures was investigated. The opal films were prepared by sedimentation of polystyrene microspheres on a cover glass. The polystyrene structures were inverted using sol-gel infiltration of silica and subsequent removal of polystyrene. Photoluminescence of rhodamine (rhodamine B, 6G and sulfo-rhodamine 101) dye solutions embedded into the inverse silica opal structures exhibited clear signatures of the lasing via a distributed feedback (DFB) and gain modulation. The refractive index contrast between the dye and the inverse opal was small enough ( $\sim 0.03\%$ ) for the formation of refractive index coupling between the lasing modes. The lasing spectrum exhibited a highly regular periodic structure of modal peaks, rather than the chaotic superposition of peaks reported in previous studies. Lasing modes having a spectral width of about 0.25 nm and a free spectral range of about 0.75 nm appeared at the position of the maximum gain (the maximum fluorescence of the dye).

© 2009 Optical Society of America

**OCIS codes:** (160.5298) Photonic crystals;(140.2050) Dye Lasers; (160.3380) Laser materials;

---

## References and links

1. V. S. Letokhov, "Generation of light by a scattering medium with negative resonance absorption," *Sov. Phys. JETP*, **26**, 835 – 840 (1968).
2. D. Wiersma, M. van Albada, and A. Lagendijk, "Coherent backscattering of light from an amplifying medium," *Phys. Rev. Lett.*, **75**, 1739 – 1742 (1995).
3. C. Vanneste, P. Sebbah, and H. Cao, "Lasing with resonant feedback in weakly scattering random systems," *Phys. Rev. Lett.*, **98**, 143902/1–4 (2007).
4. P. Anderson, "Absence of diffusion in certain random lattices," *Phys. Rev.*, **109**, 1492 – 1505 (1958).
5. S. Juodkazis, K. Fujiwara, T. Takahashi, S. Matsuo, and H. Misawa, "Morphology-dependent resonant laser emission of dye-doped ellipsoidal microcavity," *J. Appl. Phys.*, **91**, 916–921 (2002).
6. V. V. Datsyuk, S. Juodkazis, and H. Misawa, "Properties of a laser based on evanescent-wave amplification," *J. Opt. Soc. Am. B*, **22**, 1471 – 1478 (2005).
7. N. M. Lawandy, R. M. Balachandran, A. S. L. Gomes, and E. Sauvain, "Laser action in strongly scattering media," *Nature*, **368**, 436 – 438 (1994).
8. Y. Akahane, T. Asano, B. S. Song, and S. Noda, "High-Q photonic nanocavity in a two-dimensional photonic crystal," *Nature*, **425**, 944–947 (2003).
9. H. Fujiwara and K. Sasaki, "Microspherical lasing of an erbium-ion-doped glass particle," *Jpn. J. Appl. Phys.*, **41**(1A/B), L46–L48 (2002).
10. H. Fujiwara and K. Sasaki, "Lasing of a microsphere in dye solution," *Jpn. J. Appl. Phys.*, **38**, 5101 – 5104 (1999).
11. S. Frolov, Z. Vardeny, A. Zakhidov, and R. Baughman, "Laser-like emission in opal photonic crystals," *Opt. Commun.*, **162**, 241–246 (1999).

12. M. N. Shkunov, M. C. DeLong, M. E. Raikh, Z. V. Vardeny, A. Zakhidov, and R. H. Baughman, "Photonic versus random lasing in opal single crystals," *Synth. Met.*, **116**, 485 – 491 (2001).
13. R. Polson, A. Chipouline, and Z. Vardeny, "Random lasing in  $\pi$ -conjugated films and infiltrated opals," *Adv. Mater.*, **13**, 760–764 (2001).
14. R. Polson and Z. Vardeny, "Organic random lasers in the weak-scattering regime," *Phys. Rev. B*, **71**, 045205 (2005).
15. S. Yokoyama and S. Mashiko, "Tuning of laser frequency in random media of dye-doped polymer and glass particle hybride," *Jpn. J. Appl. Phys.* **42**, L970 – L973 (2003).
16. M. P. van Albada and A. Lagendijk, "Observation of weak localization of light in a random medium," *Phys. Rev. Lett.*, **55**(24), 2692 – 2695 (1985).
17. Y. Nishijima, K. Ueno, S. Juodkazis, V. Mizeikis, H. Misawa, T. Tanimura, and K. Maeda "Inverse silica opal photonic crystals for optical sensing applications," *Opt. Express*, **15**, 12979-12988 (2007).
18. Y. Nishijima, K. Ueno, S. Juodkazis, V. Mizeikis, H. Misawa, M. Mitsuru, and M. Masashi "Tunable single-mode photonic lasing from zirconia inverse opal photonic crystals," *Opt. Express*, **16**, 13676-13684 (2008).
19. A. Yariv, *Optical Electronics in Modern Communications, 5th ed.* (Oxford University Press, New York, 1997).
20. K. Yoshino, S. Tatsuhara, Y. Kawagishi, M. Ozaki, A. A. Zakhidov, and Z. V. Vardeny, "Amplified spontaneous emission and lasing in conducting polymers and fluorescent dyes in opals as photonic crystals," *Appl. Phys. Lett.*, **74**, 2590 – 2592 (1999).
21. M. N. Shkunov, M. C. DeLong, M. E. Raikh, Z. V. Vardeny, A. A. Zakhidov, and R. H. Baughman, "Photonic versus random lasing in opal single crystals," *Synth. Met.*, **116**, 485 – 491 (2001).
22. S. G. Johnson. and J. D. Joannopoulos, "Block-iterative frequency-domain methods for Maxwell's equations in a planewave basis", *Opt. Express*, **8**, 173–190 (2001).

## 1. Introduction

Recent advances in micro-photonics have demonstrated lasing in systems where optical feedback occurs due to disorder, multiple scattering, and Anderson localization [1, 2, 3, 4] rather than the usual set of discrete mirrors and distributed feedback (DFB) of other types of cavity coupling [5, 6]. Lasing in random structures [1, 3, 7, 8, 9, 10] has gained wide interest from both theoretical and applied science fields. Fluorescent dyes infiltrated into photonic crystals have been found to exhibit random lasing [11, 12, 13, 14] within the fluorescence band of the infiltrated dye, regardless of the photonic band dispersion and photonic stop-gaps; this phenomenon is considered to be common to various ordered and random media in the so-called weak scattering regime, when the free path of emitted radiation is much longer than its wavelength [14, 16]. In photonic crystals, lasing occurs with large fluctuations in amplitude and spectrum [15], and has been explained by the existence of multiple random cavities having different gain parameters and effective lengths. Interestingly, the lasing in opal photonic crystals exhibits a periodic spectral structure of narrow emission lines separated by 0.74 nm [11] attributed to stacking faults or other structural defects separated by a dominant distance of about 300  $\mu\text{m}$  in the investigated opal single-crystals. The questions of whether the randomness of the structure is essential for lasing and how it is related to the reported well-ordered lasing comb both call for further investigation.

Here, we report observations of lasing in dye-infiltrated inverse synthetic opals, with a highly regular set of narrow spectral peaks separated by  $\sim 0.75$  nm explainable by a DFB lasing mechanism. The amplitudes and spectral positions of these peaks are highly stable from measurement to measurement and sample to sample and regardless of pump power. These findings can not be due to stacking faults or other defects, because the synthetic opal samples were made by inversion from well-ordered opal templates where the single-crystal regions were more than 30  $\mu\text{m}$  in diameter and  $\sim 60$   $\mu\text{m}$  in thickness.

## 2. Experimental details

The inverse silica opal structures were obtained by the following procedures. Polystyrene microspheres with diameters of 0.2, 0.4, 0.6, 0.8, and 1  $\mu\text{m}$  and narrow size dispersion ( $\sim 0.6\%$ )

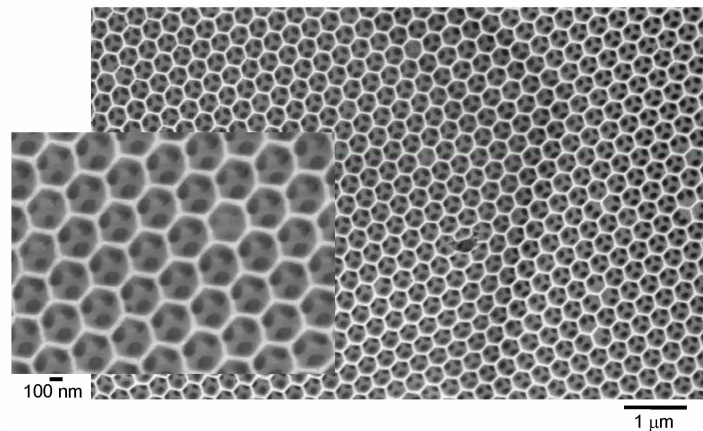


Fig. 1. SEM images of inverse opal structures formed by spheres with diameter of 300 nm showing the crystallographic (111) plane.

(Sekisui Plastics Co., Ltd.) were deposited on cover glass using centrifuged sedimentation at 5000 rpm for 10 min. The resulting direct polystyrene opal structures were dried, then annealed at 90°C for 3 min in order to produce moderate sintering of the spheres. The direct opals were subsequently inverted using a low-temperature sol-gel procedure by immersion into tetra-ethoxy silane sol [17]. The residual polystyrene was removed from the structures by washing in ethyl acetate. As a result, inverse silica opals were obtained with crystallographic (111) opal planes on the surface. Inspection of the samples was carried out by scanning electron microscopy (SEM). Film-like samples had a total thickness of 50 – 80 μm and were of a good structural quality (Fig. 1).

For optical emission measurements the samples were soaked by a 0.5 mM solution of rhodamine B, 6G, and sulfo-rhodamine 101 in ethylene glycol. The molar extinction coefficient of each dye at 532 nm wavelength was  $9.1 \times 10^5 \text{ M}^{-1}\text{cm}^{-1}$  (R6G),  $3.1 \times 10^5 \text{ M}^{-1}\text{cm}^{-1}$  (RhB), and  $1.4 \times 10^5 \text{ M}^{-1}\text{cm}^{-1}$  (SR101), respectively. The optical setup used as a pump source a frequency-doubled Nd:YAG nanosecond laser operating at the wavelength of 532 nm, repetition frequency of 10 Hz, and temporal pulse length of  $\sim 7$  ns. The laser beam was coupled into an inverted microscope (IX-71, Olympus) and focused on the sample using an objective lens having 40 times magnification and numerical aperture  $NA = 0.55$ . The sample was mounted on a translation stage attached to the microscope with (111) crystallographic planes of the inverse-opal structure normal to the optical axis of the objective lens. Emission was detected by imaging the surface of the sample via the same objective lens as was used for focusing the pump beam. The collected radiation was analyzed using a spectrometer with a grating of 1200 grooves/mm (resolution  $< 0.1$  nm) with a liquid nitrogen-cooled CCD detector. During the experiments the diameter of the pumped spot on the sample was maintained at 30 μm, comparable to the size of a typical single-crystal domain of the sample. Since this value is much larger than the diffraction-limited spot size obtainable with the used objective lens at the excitation wavelength, the excited spot size was enlarged by introducing a divergence to the laser beam prior to the microscope. Optical pumping of the samples was performed along a wide variety of directions. This circumstance should not influence the reported experimental findings, since at the low-refractive-index contrast (between  $n = 1.46$  in silica and  $n = 1.42$  in ethylene glycol), dispersion of photonic bands introduced by the periodic opal structure is negligible and for the pump beam the structure is nearly isotropic.

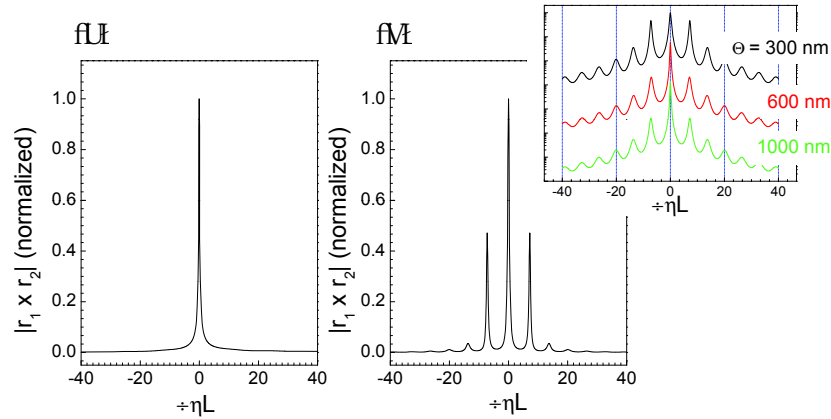


Fig. 2. (a) The gain and refractive index modulation coupled DFB lasing at single-mode conditions observed in zirconia [18]. (b) The gain-DFB modulation lasing. Simulated spectra of the DFB laser (eqn. 1);  $\Delta\beta$  is the departure of the propagation constant from the Bragg conditions  $\Delta\beta = 0$ . The inset in (b) shows spectral gain-DFB modulation for different periods  $\Lambda = 0.3, 0.8, 1.0 \mu\text{m}$  (note the log-scale in the inset).

### 3. Theory of distributed feedback lasing: gain coupling mechanism

The dye lasing phenomena in opal and inverse-opal structures can be explained by the DFB mechanism, which can take place via refractive index coupling (photonic crystal type of lasing) and gain modulation. The mixture of these two DFB lasing mechanisms has been recently reported in inverted opal zirconia structures (refractive index  $n = 2.10$ ) soaked in an ethylene glycol ( $n = 1.42$ ) dye solution [18]. The refractive index of silica opals (inverse opals) almost matches that of ethylene glycol  $n \simeq 1.42$ . Such structures can be used to realize a gain-DFB mechanism and is the subject of the present study.

A one-dimensional DFB mechanism can be realized when the cumulative reflection coefficients  $r_{1,2}$  over the length  $L$  of a periodic structure are [19]:

$$r_{1,2}(L_{1,2}) = \frac{\kappa \sinh SL_{1,2}}{(\gamma - i\Delta\beta) \sinh SL_{1,2} - S \cosh SL_{1,2}}, \quad (1)$$

where  $L_{1,2}$  denotes an arbitrary position inside the cavity satisfying relation  $L_1 + L_2 = L$  where  $L$  is the total length of the cavity (for simulations  $L_{1,2} = L/2$  was implemented),  $S = \sqrt{\kappa^2 + (\gamma - i\Delta\beta)^2}$ ,  $\Delta\beta = \frac{\omega}{c} n_{mode} - \frac{\pi}{\Lambda}$ ,  $n_{mode}$  is the effective refractive index of the mode propagating along the DFB structure, and  $\kappa = \frac{\pi n_1}{\lambda} + i\frac{\gamma_1}{2}$  is the generalized coupling constant accounting for the both the refractive and gain modulation. The modulations of the refractive index  $n$ , and gain  $\gamma$  (a negative absorption) are given by:

$$n(z) = n_0 + n_1 \cos \frac{2\pi}{\Lambda} z, \quad (2)$$

$$\gamma(z) = \gamma_0 + \gamma_1 \cos \frac{2\pi}{\Lambda} z, \quad (3)$$

where the  $\Lambda$  is the period of the modulation along the DFB structure on the cavity coordinate  $z$ . When reflections of the forward and backward waves satisfy  $|r_1 \times r_2| \geq 1$ , lasing occurs. It

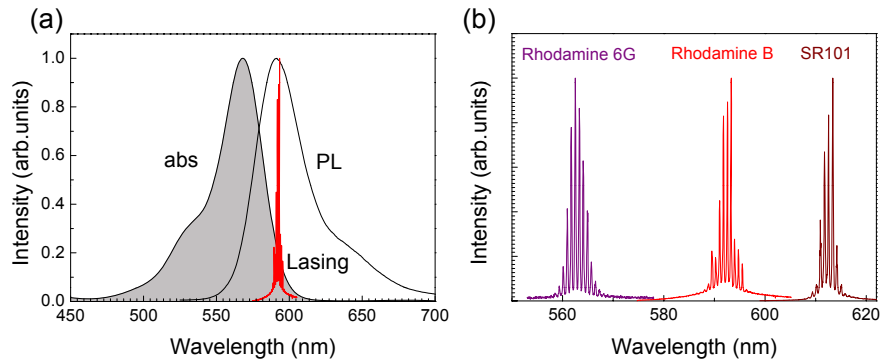


Fig. 3. (a) Spectra of rhodamine B absorption, fluorescence, and lasing lines measured from a silica inverse opal film at a pump irradiance of  $157 \text{ GW/cm}^2$  per pulse. (b) Lasing modes from inverse opal film infiltrated by different dyes. The mode of spectral spacing is approximately the same.

should be noted that this model considers the simple case of uniform gain and refractive index modulation over the entire length of the cavity.

In experiments, the lasing spectrum was not dependent on the excitation spot size (provided the pump fluence was kept the same). The effective absorption depth in a high-concentration dye should be related to the cavity length,  $L$ , used in simulations. However, the exact correspondence between the effective absorption length and the length  $L$  is difficult to determine since the model is 1D while the actual structure is 3D. Also, in simulations the factor  $\Delta\beta L$  enters equations as an argument (the shorter length can be compensated by a larger propagation constant and vice versa).

When both refractive index and gain mechanisms take place simultaneously there is a spectral competition between lasing at the stop gap edges (refractive index DFB) and the Bragg wavelength (center of stop gap). In zirconia-inverted opals soaked in ethylene glycol rhodamine solutions this interplay of mechanisms resulted in unique single-mode lasing [18] as simulated in Fig. 2(a). The spectral position was close to the maximum of dye photoluminescence (PL) even when its spectral position was within the stop-gap. The exact lasing wavelength was determined via the spectral profile of the gain (the PL band) and the spectral profile of the DFB.

The pure gain-DFB is realized when  $n_1 \rightarrow 0$  and the gain modulation  $\gamma_1$  is responsible for the feedback. The lasing peaks are expected around the Bragg wavelength as shown in Fig. 2(b). It is noteworthy that the peak separation is independent for the period  $\Lambda$  of the structure as shown by simulations in the inset of Fig. 2(b) for the several periods used in our experiments on silica inverted opals. This corresponded well to our experimental observations (see, Sec. 4) and to results reported in opals [11]. Values of the refractive index and gain modulation were experimentally determined for the  $\langle 111 \rangle$  direction: the average refractive index was 1.44 with modulation of 0.03% obtained from calculations of the space-filling factors of silica and ethylene glycol. The multi-peak tendency of the lasing comb remained present when the index modulation was in the range from 0% to 0.2% in our calculation. The gain value was fixed to the known absorption coefficient calculated for the used concentration (see the experimental section).

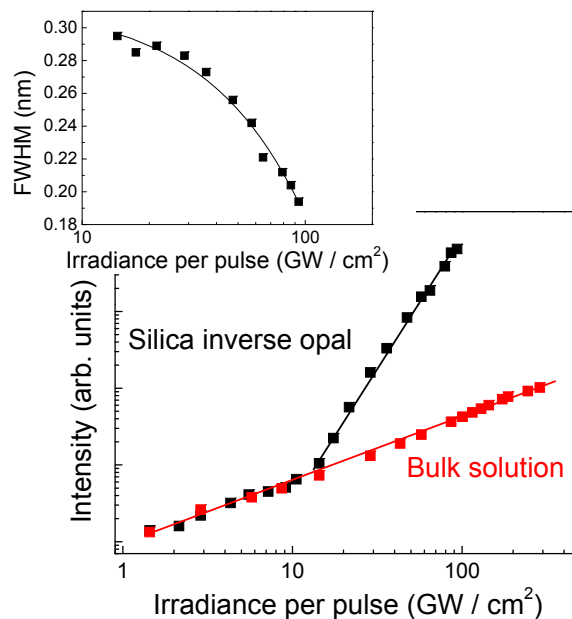


Fig. 4. Intensity dependence of the lasing maximum peak from the inverse silica film doped by rhodamine B dye. The inset shows the power dependence of the spectral narrowing of the emission modes.

#### 4. Results and discussion

Unless stated otherwise, the following discussion concentrates on inverse-opal structures, templated from microspheres with diameter of 300 nm. Figure 3(a) compares the dye absorption and emission lines above and below the lasing threshold in silica inverse opal films. As can be seen, the lasing line is spectrally narrower than the PL line and is coincident with peak PL, where the optical gain is the highest. One can readily discern the presence of finer features within the lasing line. The typical spectral shape of the lasing emission consisting of a series of sharp peaks is shown with higher resolution in Fig. 3(b). Lasing emission is strongly linearly polarized, with intensity ratio between parallel and perpendicular polarization components  $I_{\parallel}/I_{\perp} \simeq 66$  (the parallel component is polarized along the polarization of pump pulse). The lasing spectra of two other dyes (R6G and SR101) infiltrated into the same opal sample are also shown in Fig. 3(b). It can be easily verified that in these dyes the spectral position of the lasing emission follows that of the peak PL. The influence of photonic stop gaps and band dispersion on the lasing can be ruled out completely due to the negligible refractive index contrast between ethylene glycol and silica (1.42 vs. 1.46).

The photonic band diagrams of a closely-packed opal structure consisting of materials with specific refractive indexes was calculated using MIT-Photonic-Bands software package[22]. These calculations have demonstrated the absence of photonic stop gaps, thus supporting our earlier assumption.

The power dependence of the emission and the bandwidth of lasing modes are illustrated in Fig. 4. The emission power exhibits a transition from a linear to a super-linear regime. This transition is accompanied by a spectral narrowing of the emission shown in the inset of Fig. 4. A transition of the dye's PL from the amplified spontaneous emission into the typical lasing spectrum with well-defined modes was observed at approximately 20 GW/cm<sup>2</sup> irradiance. At

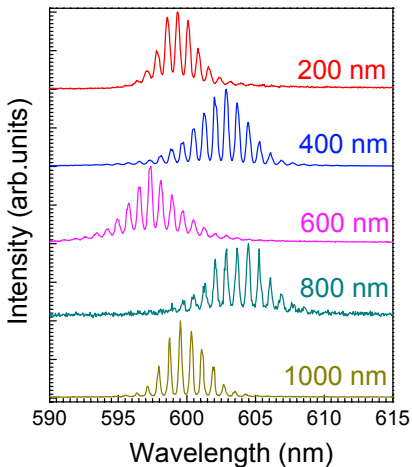


Fig. 5. Lasing of rhodamine B in inverse opal structures templated from polystyrene beads of different diameters.

this irradiance, the spectral narrowing of the modes was accompanied by an exponential growth of their intensity, which is a signature of lasing. At the maximum pump irradiance, the spectral width of the lasing modes,  $\sim 0.19$  nm, was only slightly larger than the instrumental response of the used spectrometer, 0.1 nm.

The periodic modulation seen in the lasing modes (Fig. 5) appeared at a higher resolution for silica inverse opal films templated from spheres having diameters of  $0.2 - 1 \mu\text{m}$ . Regardless of the lattice period, the lasing peaks have a spectral half-width of about 0.25 nm, and a spectral separation of  $\Delta\lambda = 0.77$  nm. All the spectra were taken at the pumping power approximately 15% above the lasing threshold. The same intra-mode spectral spacing was observed in opal films soaked with dyes (without inversion), only at a slightly lower lasing threshold.

Although spectral positions of lasing modes vary from sample to sample according to Fig. 5, their width and spectral separation is nearly constant. This can be illustrated by calculating a power Fourier transform of the spectra (not shown here). We can infer dominance of a single effective cavity in all of the investigated inverse-opal structures. In earlier reports, random lasing was found to possess much more chaotic spectral shapes and contain more harmonics.

For different samples with the same lattice period, spectral positions of the lasing peaks were found to be constant within about 0.2 nm. The maximum deviation from the average peak wavelength does not exceed the separation between different peaks. The spectral positions of the lasing modes were also found to be independent of the pump power, an attractive feature for applications.

Thus, our findings illustrate the presence of the same cavity responsible for the gain-DFB lasing and is qualitatively well supported by modeling (Sec. 3). One may suspect that the discrete spectral peaks might have come from cavities formed by multiple reflections at the boundaries of the samples or at various extended defects inside the samples. However, essentially the same behavior was observed in thin (tens-of- $\mu\text{m}$ ) samples, and in thick ( $> 100 \mu\text{m}$ ) inverse opal films at different excitation spot sizes. Therefore one can rule out shapes and structural defects as the possible reasons for our observations.

## 5. Conclusions

Lasing from dye solutions infiltrated into inverse silica opal structures was found to exhibit lasing action due to the gain-DFB mechanism. The independence of the spectral separation between lasing peaks from the period of the structure is explained by the pure gain-DFB. In contrast to most of the existing reports, the lasing spectrum was found to be highly regular, reproducible, and polarized with a series of spectral peaks having a width of about 0.25 nm and a free spectral range of about 0.75 nm. Inverse opal films are attractive for micro-laser and photonic applications since the volume fraction of the infiltrated dyes are almost three times that of opal films.

## Acknowledgments

This work was supported by funding from the Ministry of Education, Culture, Sports, Science, and Technology of Japan: KAKENHI Grant-in-Aid (No. 19049001) for Scientific Research on the Priority Area "Strong Photon-Molecule Coupling Fields for Chemical Reactions" (No. 470), Grant-in-Aid from Hokkaido Innovation through Nanotechnology Support (HINTS), and Grant-in-Aid for JSPS Fellows.